

Various Strategies to Control the Conformation of Peptoids

Claude Taillefumier, Sophie Faure, Maha Rzeigui, Maxime Pypec, Olivier Roy
Université Clermont Auvergne, Clermont Auvergne INP, CNRS, ICCF, F-63000 Clermont–Ferrand, France

Introduction

N-substituted glycines oligomers or peptoids have drawn considerable interest as peptide biomimetics [1]. They possess many desirable attributes such as *in vivo* stability, ease of synthesis, and side chain diversity. Peptoids are also a special class of foldamers, as both *cis*- and *trans*-amide bond conformations are accessible. In this respect, peptoids show similarities to proline-rich sequences. For example, they can adopt type I (PPI) and type II (PPII) helical conformations. This involves regulating amide isomerism in the peptoid backbone. Considerable efforts have been made to control the conformation of peptoids through steric and electronic interactions involving peptoid amides and nearby side chains. Among the best *cis*-amide inducing side chains are the *N* α -chiral aromatic phenylethyl, naphthylethyl and triazolium groups, or the alkyl-ammonium, fluorinated and *tert*-butyl side chains (Figure 1A). Fewer side chains are capable of promoting *trans* peptoid amides. Among these, are the *N*-aryl, *N*-hydroxy, *N*-alkoxy, *N*-acylhydrazide, *N*-imino and *N*-alkylamino groups (Fig. 1B). All these findings are recapitulated in a recent review by Kalita *et al.* [2]. Here we report on our results with the following two sterically demanding aliphatic side chains, *tert*-butyl (*t*Bu) and (*S*)-1-*tert*-butyl(ethyl) (*s*1tbe), which our group has introduced to the peptoid “tool box” to induce *cis*-amides. In particular, the modulation of peptoid helicity by sequence specific positioning of chiral (*N**s*1tbe) and achiral monomers (*N**t*Bu) will be discussed [3,4]. We will also consider the conformation of homologous β -peptoid oligomers bearing *N**t*Bu side chains.

Results and Discussion

We first showed in 2013 that the bulky *tert*-butyl side chain is able to freeze peptoid amide-bonds in the *cis* conformation [5]. We then demonstrated that achiral *Nt*Bu-glycine homo-oligomers can preferentially adopt helical folding as a result of weak intramolecular non-covalent interactions, of which some are specific to the *tert*-butyl group (*t*Bu...*t*Bu London interactions) [6]. These results led us to look for another highly congested aliphatic side chain, but this time with a chiral center to control helix handedness. This is how the (*S*)-1-*tert*-butyl(ethyl) side chain (*s*1tbe) was introduced to the peptoid ‘toolbox’ [7]. Two families of peptoids (A and B) are presented here. The A family comprises the homo-oligomers Ac-(*Ns*1tbe)_{*n*}-*Ot*Bu ranging from monomer to nonamer (Table 1). The B family corresponds to mixed peptoid oligomers comprising *Nt*-*tert*-butylglycine (*Nt*Bu) and α -chiral (*S*)-*N*-(1-*tert*-butyl(ethyl)glycine residues (*Ns*1tbe) (Table 2). The principle of the submonomer solution-phase synthesis which we adopted to prepare the peptoid molecules is shown in Figure 2. For each oligomer, we determined by integration of the NMR spectra (CDCl₃, CD₃CN and CD₃OD) the overall proportion of *cis* and *trans* rotamers, expressed as the $K_{cis/trans}$ ratio in Tables 1 and 2.

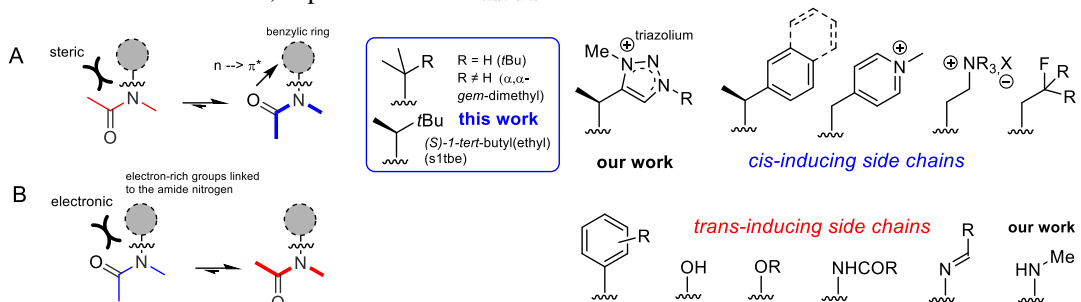


Fig. 1. Key interactions that regulate peptoid amide bond isomerism and summary of the most structuring side chains.

Table 1. Sequences of peptoids **1-9** (Family A) and overall backbone $K_{cis/trans}$ values as determined by 1H NMR spectra integration in $CDCl_3$, CD_3CN and CD_3OD .

peptoid	sequence	$CDCl_3$	CD_3CN	CD_3OD
		$K_{cis/trans}$	$K_{cis/trans}$	$K_{cis/trans}$
1	Ac- <i>Ns</i> 1tbe-OtBu	0.64	0.67	0.77
2	Ac-(<i>Ns</i> 1tbe) ₂ -OtBu	0.98	1.60	1.68
3	Ac-(<i>Ns</i> 1tbe) ₃ -OtBu	1.95	2.61	3.00
4	Ac-(<i>Ns</i> 1tbe) ₄ -OtBu	>19	10.89	>19
5	Ac-(<i>Ns</i> 1tbe) ₅ -OtBu	18.92	7.96	>19
6	Ac-(<i>Ns</i> 1tbe) ₆ -OtBu	>19	10.39	>19
7	Ac-(<i>Nsch</i>) ₆ -OtBu	2.71	1.39	
8	Ac-(<i>Ns</i> 1tbe) ₈ -OtBu	>19	8.08	>19
9	Ac-(<i>Ns</i> 1tbe) ₉ -OtBu	>19	12.13	>19

Family A. Table 1 shows a dramatic increase in $K_{cis/trans}$ between trimer **3** and tetramer **4** from 1.95 to >19 in $CDCl_3$, for example, which means that overall the *trans* rotamer population has decreased from 66% to <4%. The conversion of the trimer to a tetramer thus induces a dramatic increase in conformational order and suggests cooperative folding with chain elongation. The comparison of the $K_{cis/trans}$ values of hexamers **6** ($^{CDCl_3}K_{cis/trans} > 19$) and **7** ($^{CDCl_3}K_{cis/trans} = 2.71$) clearly shows the remarkable *cis*-promoting effect of the s1tbe side chain with respect to the cyclohexylethyl side chain (sch, Figure 2), which has long been considered as a reference. We were able to obtain suitable crystals of compound **5** for X-ray diffraction analysis. In the crystal, peptoid **5** adopts the structure of a nascent right-handed helix with torsion angles consistent with the PPI helix. The solution conformation of this family of peptoids was then investigated by circular dichroism (CD) which confirmed the helical conformation observed in the crystalline state. The CD spectra of peptoids **5**, **6**, **8** and **9** have a similar shape with two negative maxima at about 188 and 225 nm and an intense positive maximum at about 209 nm and an intense positive maximum at about 209 nm characteristic of the PPI helix (Figure 3). The length-dependent increase in per-amide molar ellipticity (MRE) suggests that helix folding of *Ns*1tbe oligomers is probably a cooperative process. The comparison of the intensities of the curves of the two hexamers **6** (*Ns*1tbe) and **7** (*Nsch*), clearly shows that peptoid **7** displays a greater extent of backbone flexibility. This again demonstrates the superiority of the s1tbe side chain over other aliphatic side chains. We then set out to improve the conformational stability of the *Ns*1tbe oligomers and designed a second series of oligomers (Family B) whose sequences incorporate one or more *Nt*Bu units allowing the relevant amides to be fully *cis*.

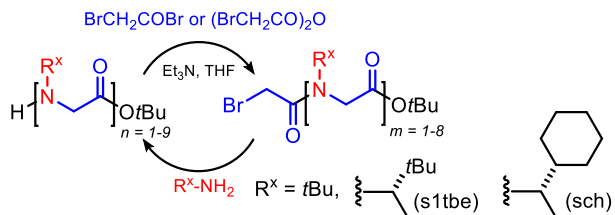


Fig. 2. Submonomer solution-phase synthesis of α -peptoids oligomers

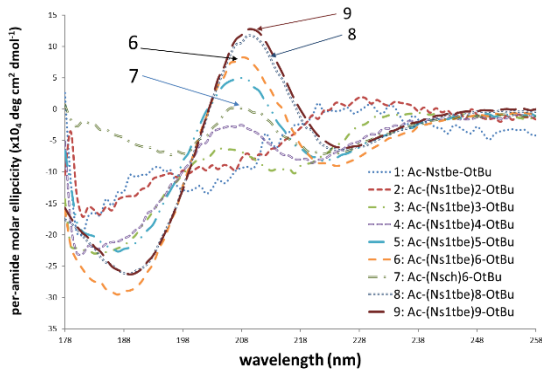


Fig. 3. CD spectra of peptoids **1-9** at 500 mM, in CH_3CN

Table 2. Sequences of peptoids **10-20** (Family B) and overall $K_{cis/trans}$ values as determined by 1H NMR/2D HSQCAD spectra integration in $CDCl_3$, and CD_3CN .

Peptoid	Sequence	$CDCl_3$	CD_3CN
		$K_{cis/trans}$	$K_{cis/trans}$
10	Ac-Ns1tbe-Ns1tbe-Ns1tbe-Ns1tbe-Ns1tbe-NtBu-OrBu	> 49	> 49
11	Ac-Ns1tbe-Ns1tbe-Ns1tbe-Ns1tbe-NtBu-Ns1tbe-OrBu	> 15.2	> 11.7
12	Ac-Ns1tbe-Ns1tbe-Ns1tbe-NtBu-Ns1tbe-Ns1tbe-OrBu	> 14.6	> 10.2
13	Ac-Ns1tbe-Ns1tbe-NtBu-Ns1tbe-Ns1tbe-Ns1tbe-OrBu	> 18.8	> 10.5
14	Ac-Ns1tbe-NtBu-Ns1tbe-Ns1tbe-Ns1tbe-Ns1tbe-OrBu	> 14.5	> 11.8
15	Ac-NtBu-Ns1tbe-Ns1tbe-Ns1tbe-Ns1tbe-Ns1tbe-OrBu	> 20.3	> 13.4
16	Ac-NtBu-Ns1tbe-Ns1tbe-Ns1tbe-Ns1tbe-NtBu-OrBu	> 23.3	> 23.3
17	Ac-NtBu-NtBu-Ns1tbe-Ns1tbe-NtBu-NtBu-OrBu	> 29.1	> 27.8
18	Ac-NtBu-NtBu-Ns1tbe-Ns1tbe-Ns1tbe-NtBu-NtBu-OrBu	> 49	> 42.0
19	Ac-NtBu-NtBu-Ns1tbe-Ns1tbe-Ns1tbe-Ns1tbe-NtBu-NtBu-OrBu	> 25.5	> 25.5
20	Ac-NtBu-NtBu-NtBu-Ns1tbe-Ns1tbe-Ns1tbe-NtBu-NtBu-NtBu-OrBu	> 49.0	> 49.0

Family B. The first finding from the comparison of the $K_{cis/trans}$ values (Table 2) of peptoid hexamers **10-15** is that the positioning of a single *cis*-promoting NtBu residue at the carboxy terminus proves exceptionally efficient to suppress the *trans*-amide rotamers. This is consistent with the known fact that the C-terminus of the PPI peptoid helix is structurally more flexible than the N-terminus [8]. The second major finding is that peptoid oligomers containing a central chiral segment of 2 to 4 consecutive Ns1tbe residues, surrounded by NtBu residues (**16-20**) display the higher overall $K_{cis/trans}$ (% *cis* = 96-100). In contrast, the incorporation of NtBu monomers every two Ns1tbe residues (not shown) does not ensure the complete suppression of peptoid amide *cis-trans* isomerism.

The strongest CD intensity (208 nm) of hexamer **10** within the group of peptoids **10-15** (Figure 4A) is consistent with an all *cis*-amide backbone ($K_{cis/trans} > 49$ in $CDCl_3$ and CD_3CN). Comparison of the CD curves of hexamers **10-15** shows that the ellipticity decreases with increasing the distance of the NtBu residue from the carboxy terminus. Also of note is that a single NtBu residue, strategically placed at the C-terminus, provides a much more stable helical conformation than a homo-oligomeric sequence of the same length (compound **10** vs hexamer Ac-(Ns1tbe)₆-OrBu).

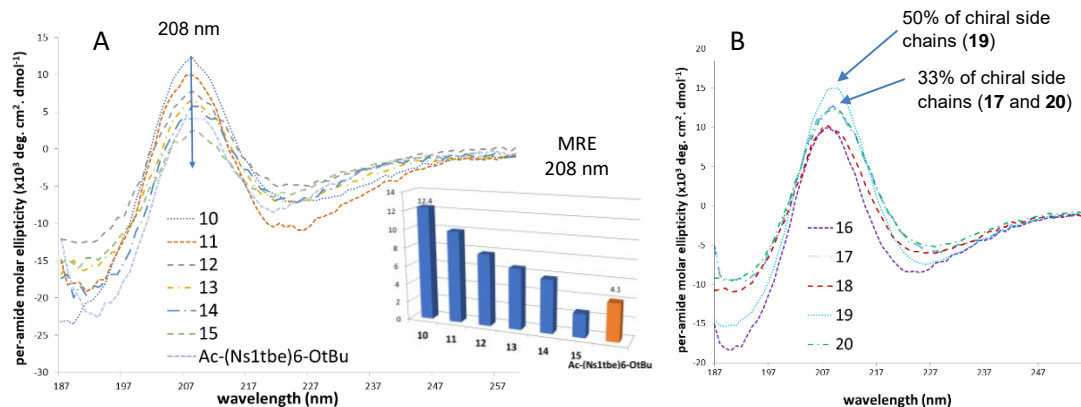


Fig. 4. CD spectra of peptoids **10-20** and reference compound Ac-(Ns1tbe)₆ in MeOH.

Regarding the DC curves of peptoids **16-20** (Figure 4B), the most striking observations are the following: the MRE of peptoid **17** is remarkable, considering its short length (hexamer) and low proportion of chiral side chains (33%). The MRE intensity of peptoid **17** at 208 nm is at the same level as that of hexamer **10**, which contains 83% of chiral side-chains. In addition, the CD spectrum of **17** in methanol has comparable shape and intensity to that of the nonamer **20**, also composed of only 33% of chiral residues. The design principle underlying the preparation of compounds **16-20** is thus particularly attractive for attaining stable helical folding with a low content of chiral side chains. The results suggest a sergeants-and-soldiers behaviour, with the central chiral segment imposing its handedness on both ends of the oligomers. This is clearly seen in the crystallographic structure of octamer **19**, the longest linear α -peptoid ever analysed in the crystal state. The structure of **19** is a right-handed PPI-like helix of great regularity despite a chiral content of only 50%.

In continuation of this work, we focused on β -*Nt*Bu oligomers and showed that they can adopt a helical structure with about three residues per turn as already described in the literature [9]. We also proposed a new regular ribbon-like structure [10].

Acknowledgments

Part of this work was supported by a grant overseen by the French National Research Agency project ARCHIPEP. M.Rzeigui was supported by a grant from the Ministry for Higher Education and Scientific Research of Tunisia, and M. Pypec by a grant of University Clermont-Auvergne. We would like to acknowledge Aurélie Job (HPLC) and Martin Lereboure (mass spectrometry) for their assistance. We also acknowledge the UMS2008-IBSLor Biophysics and Structural Biology core facility at Université de Lorraine for CD measurements.

References

1. Horne, W.S. *Expert Opin Drug Discov.* **6**, 1247-1262 (2011), <https://doi.org/10.1517/17460441.2011.632002>
2. Kalita, D., et al. *Chem. Asian J.* e202200149 (2022), <https://doi.org/10.1002/asia.202200149>
3. Shin, H., et al. *Chem. Commun.* **50**, 4465-4468 (2014), <https://doi.org/10.1039/C3CC49373C>
4. Rzeigui, M., et al. *J. Org. Chem.* **85**, 2190-2201 (2020), <https://doi.org/10.1021/acs.joc.9b02916>
5. Roy, O., et al. *Org. Lett.* **15**, 2246-2249 (2013), <https://doi.org/10.1021/ol400820y>
6. Angelici, G., et al. *Chem. Commun.* **52**, 4573-4576 (2016), <https://doi.org/10.1039/C6CC00375C>
7. Roy, O., *J. Am. Chem. Soc.* **139**, 13533-13540 (2017), <https://doi.org/10.1021/jacs.7b07475>
8. Wu, C.W. *J. Am. Chem. Soc.* **123**, 6778-6784 (2001), <https://doi.org/10.1021/ja003154n>
9. Laursen, J.S. *Nat Commun* **6**, 7013 (2015), <https://doi.org/10.1038/ncomms8013>
10. Angelici, G., et al. *Org. Biomol. Chem.* 2022, Accepted Manuscript, <https://doi.org/10.1039/D2OB01351G>

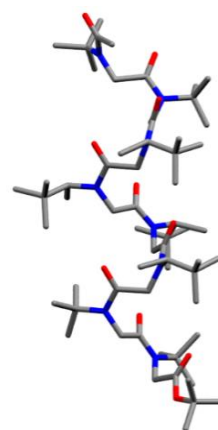


Fig. 5. X-ray structure of octamer **19**.